AGU PUBLICATIONS

Geophysical Research Letters

RESEARCH LETTER
10.1002/2014GL059361

Key Points:
- Twelve thousand year record of Nile River discharge and East African monsoon evolution
- Three thousand five hundred year period of gradual middle to late Holocene transition of East African monsoon
- Synchronous pacing of middle to late Holocene hydroclimate and vegetation changes

Supporting Information:
- Readme
- Text S1

Correspondence to:
S. Weldeab,
weldeab@geol.ucsb.edu

Citation:
Weldeab, S., V. Menke, and G. Schmiedl (2014), The pace of East African monsoon evolution during the Holocene, *Geophys. Res. Lett.*, *41*, 1724–1731, doi:10.1002/2014GL059361.

Received 21 JAN 2014
Accepted 18 FEB 2014
Accepted article online 20 FEB 2014
Published online 10 MAR 2014

The pace of East African monsoon evolution during the Holocene

Syee Weldeab[1], Valerie Menke[2], and Gerhard Schmiedl[2]

[1]Department of Earth Science, University of California, Santa Barbara, California, USA, [2]Center for Earth System Research and Sustainability, University of Hamburg, Hamburg, Germany

Abstract African monsoon precipitation experienced a dramatic change in the course of the Holocene. The pace with which the African monsoon shifted from a strong early to middle to a weak late Holocene is critical for our understanding of climate dynamics, hydroclimate-vegetation interaction, and shifts of prehistoric human settlements, yet it is controversially debated. On the basis of planktonic foraminiferal Ba/Ca time series from the eastern Mediterranean Sea, here we present a proxy record of Nile River runoff that provides a spatially integrated measure of changes in East African monsoon (EAM) precipitation. The runoff record indicates a markedly gradual middle to late Holocene EAM transition that lasted over 3500 years. The timing and pace of runoff change parallels those of insolation and vegetation changes over the Nile basin, indicating orbitally forced variation of insolation as the main EAM forcing and the absence of a nonlinear precipitation-vegetation feedback. A tight correspondence between a threshold level of Nile River runoff and the timing of occupation/abandonment of settlements suggests that along with climate changes in the eastern Sahara, the level of Nile River and intensity of summer floods were likely critical for the habitability of the Nile Valley (Egypt).

1. Introduction

The notion of a vast landscape with a lavish grassland and seasonally migrating megafauna in today's most hostile, hyperarid Sahara just 4000–5000 years ago captivates the general public and scientists alike [*Claussen and Gayler*, 1997; *Gasse*, 2000]. The abruptness or the pace of the hydroclimatic shifts during the middle to late Holocene African monsoon transition and its coupling with vegetation changes are, however, controversially debated [*Brovkin and Claussen*, 2008; *Claussen et al.*, 2013; *deMenocal et al.*, 2000; *Kroepelin et al.*, 2008]. Inconsistency between various climate records and the associated debate is not limited to the northernmost margin of the monsoon system but includes the core area of the East African monsoon (EAM). Reconstruction of dust flux off northwest Africa indicates an abrupt increase of dust mobilization in Western Sahara during the middle to late Holocene transition [*deMenocal et al.*, 2000]. In contrast, lake records from the central Sahara and dust accumulation in the eastern Mediterranean Sea (EMS) reveal a gradual transit of hydroclimate changes and increase of Saharan dust mobilization, respectively [*Box et al.*, 2011; *Ehrmann et al.*, 2013; *Kroepelin et al.*, 2008]. Similarly, in the core area of EAM, hydroclimate, vegetation, and dust records show a markedly progressive shift from a wet, tree- and shrub-dominated vegetation and less dusty middle Holocene to a late Holocene marked by relatively reduced precipitation, development of grassland, and increase in dust mobilization [*Berke et al.*, 2012; *Foerster et al.*, 2012; *Jung et al.*, 2004; *Kendall*, 1969; *Marshall et al.*, 2011; *Stager et al.*, 2003]. In strong contrast to the above findings, other records from the EAM area suggest an abrupt middle to late Holocene transition [*Garcin et al.*, 2009; *Tierney and DeMenocal*, 2013].

Here we present a spatially integrated hydroclimate record of the East African monsoon (EAM) core area, providing detailed insights into the evolution and pace of EAM precipitation changes throughout the Holocene. We focus on a sediment sequence retrieved from the eastern Mediterranean Sea (EMS), directly under the influence of Nile River freshwater input (Figure 1). Prior to the construction of the High Dam at Aswan in 1965, summer (July–September) Nile River runoff amounted to up to 54 km^3/yr and had a strong impact on the surface salinity, nutrient availability, and dissolved trace elements over the core site, with salinity varying from preflood values of 39 practical salinity units (psu) down to 33 psu during flooding season [*Hecht*, 1992]. The Nile River drains a basin of 3.1 million km^2 and has an annual discharge of 90 ± 17 km^3/yr with peak values (22 ± 4 km^3/month) occurring during September. Most of the seasonal precipitation occurs over the Blue Nile River basin between June and September and over the White Nile basin with a biannual precipitation pattern (see Figure 1 for more details). The moisture that advects from the western Indian Ocean

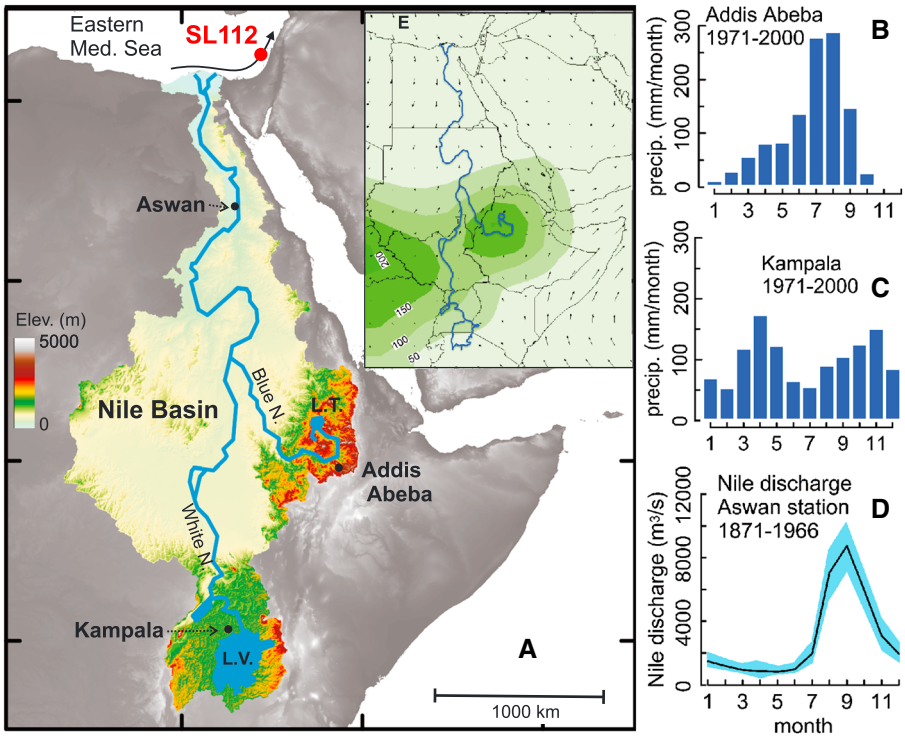

Figure 1. (a) Topographic map of the Nile basin (color shade); L.T. and L.V. denote Lake Tana and Lake Victoria, respectively. Red dot and arrow in the eastern Levantine basin indicate the SL112 location and the direction of surface current. Monthly rainfall over (b) Addis Abeba and (c) Kampala representing the Blue Nile and White Nile river catchments, respectively (averaged values of data collected between 1971 and 2000; data source: World Meteorological Organization, http://worldweather.wmo.int). (d) Monthly Nile River discharges between 1871 and 1966 showing peak discharge in September ($8745 \pm 1636\ m^3/s$ corresponding to $22.8 \pm 4.2\ km^3$/month); black line and blue area indicate monthly mean discharge values and the deviation from the mean value, respectively (data from River Discharge Database, http://www.sage.wisc.edu/riverdata). (e) Climatology over Eastern Africa and adjacent region. In Figure 1b, contours and number show rainfall in August (mm/month), and arrows indicate strength and direction of wind field at 925 mbar during August (data from http://iridl.ldeo.columbia.edu). Figures 1b and 1c demonstrate that the seasonal variation of the modern Nile River discharge is largely controlled by seasonal changes in precipitation over the Blue Nile River basin.

and the Congo basin/Atlantic Ocean into the Nile basin is controlled by the seasonal shift of the Intertropical Convergence Zone and Congo Air Boundary [*Costa et al.*, 2014]. According to *Costa et al.* [2014], 69–95% and 5–24% of precipitation over Lake Tana is fed by moistures originating from the western Indian Ocean and the Congo basin/Atlantic Ocean, respectively.

We use Ba/Ca in *Globigerinoides ruber* pink, a surface-dwelling and low-salinity-tolerating species [*Ufkes et al.*, 1998], as a novel proxy for runoff-induced EMS surface freshening and hence hydroclimate reconstruction of the Nile basin. Runoff of tropical rivers is highly enriched in dissolved Ba (Ba_{dis}) varying between 140 and 350 nmol/kg [*Bahr et al.*, 2013] relative to Ba concentration of open ocean seawater (35–40 nmol/kg) [*Bahr et al.*, 2013; *Edmond et al.*, 1978]. Despite varying geology of the catchments, vegetation cover, and weathering type, data compilation shows that Ba_{dis} off several tropical river systems is primarily controlled by the amount of runoff [*Bahr et al.*, 2013]. The uptake of Ba_{dis} into foraminiferal calcite is linearly correlated to the amount of dissolved Ba in the water in which the species calcify [*Bahr et al.*, 2013; *Hönisch et al.*, 2011; *Lea and Spero*, 1994]. Furthermore, foraminiferal Ba uptake is independent of changes in calcification temperature and alkalinity [*Hönisch et al.*, 2011], and Ba is homogenously distributed within the foraminiferal calcite (supporting information). These observations make Ba/Ca in *G. ruber* a critical tool for reconstructing catchment hydrology [*Saraswat et al.*, 2013; *Sprovieri et al.*, 2012; *Weldeab*, 2012; *Weldeab et al.*, 2007, 2011]. Our work has several crucial advantages and provides unprecedented insights into the EAM evolution. Previous reconstruction of Nile discharge relied on $\delta^{18}O_{G.\ ruber}$ and detrital components of EMS marine sediment [*Almogi-Labin et al.*, 2009; *Hamann et al.*, 2009; *Rohling et al.*, 2002]. The former harbors several components unrelated to the amount of

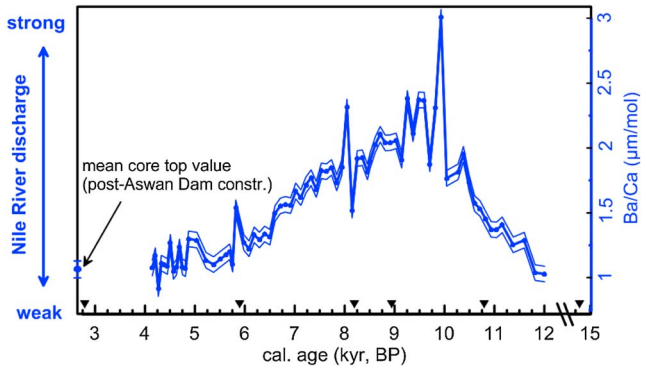

Figure 2. Bold blue line indicates Ba/Ca time series analyzed in surface-dwelling planktonic foraminifers *Globigerinoides ruber* variety pink (250–300 µm) from core sediment SL112. Thin blue lines indicate Monte Carlo simulation-based estimate of analytical and sampling uncertainty band at 95% confidence level. Mean value (1.07 ± 0.06 µmol/mol, $n = 15$) of off Nile core top samples is indicated on the left *y* axis. Triangle symbols along the time axis indicate age control points based in radiocarbon measurements and EMS-wide events (see supporting information).

runoff, including calcification temperature and changes in the isotope signatures of precipitation. Riverine sediment load and its manifestation in marine sediment sequences can be modulated by erosion (unrelated to amount of precipitation) and sedimentary dilution, respectively. The $Ba/Ca_{G.ruber}$ record is independent of changes in sedimentation rate and degradation/preservation issues that influence proxies analyzed in bulk sediment. Furthermore, in contrast to $\delta^{18}O_{seawater}$ (reconstructed from $\delta^{18}O_{G.\,ruber}$) and δD of leaf wax that at times harbor isotope imprints unrelated to changes in the amount of precipitation [*Costa et al.*, 2014; *Weldeab*, 2012], $Ba/Ca_{G.\,ruber}$ primarily reflects the degree of surface freshening, and by extension changes in the amount of precipitation. Our Ba/Ca record provides a spatially integrated measure of hydroclimate changes in the Nile basin and puts the timing of the occupation and abandonment of prehistoric settlements in the Nile Valley (Egypt) into the context of the intensity of summer Nile River floods.

2. Materials and Methods

We generated a time series of Ba/Ca in *G. ruber* pink from sediment core SL112 retrieved from the eastern Levantine basin (32°44.5′N, 34°39.0′E, water depth 892 m) underneath the Nile River freshwater pathway (Figure 1). Sample preparation and Ba/Ca analysis were carried out following the University of California, Santa Barbara standard cleaning method [*Martin and Lea*, 2002] and using inductively coupled plasma–mass spectrometry (ICP-MS) (Element 2), respectively. Analytical uncertainty accounts for ±0.04 µmol/mol. The record covers the time window between 4 and 12 thousand calendar years before present (kyr cal B.P.). The age model is constrained by previously published radiocarbon dates, tephra layer, and the timing of well-dated EMS-wide events [*Hamann et al.*, 2010; *Schmiedl et al.*, 2010] (see supporting information for detailed information).

3. Results

Consistent with the low amount of Nile River freshwater reaching the Levantine basin and hence low dissolved Ba in surface water (59.4 ± 1.4 nmol/kg corresponding to Ba/Ca of 5.2 ± 0.1 µmol/mol) [*Lea*, 1990], Ba/Ca in Rose Bengal-stained *G. ruber* pink in Levantine core top samples is low (1.07 ± 0.06 µmol/mol, $n = 15$) (Figure 2). Starting from low pre-Holocene values, Ba/Ca gradually increased and reached the highest Ba/Ca values (2.14 ± 0.3 µmol/mol, $n = 12$) during the early Holocene. A progressive decline in Ba/Ca started at 7.8 kyr cal B.P. and reached Ba/Ca ratios that are, on average, similar to the core top values at 4–4.8 kyr cal B.P. (Figure 2). Centennial-scale decline of Ba/Ca is recorded at 8.2–8.4 kyr cal B.P. and 10.2 kyr cal B.P. Because the centennial features are represented by only few data points and model uncertainties at this resolution, we focus on the millennial-scale trend.

4. Discussion

We interpret the variation of Ba/Ca to primarily reflect changes in Nile River discharge and hence hydroclimate changes over the Nile basin that constitutes the core area of the East African monsoon. Prior to the construction of the High Dam at Aswan in 1965, seasonal Nile River discharge of up to 56 km^3 was diverted directly over our core site and left a strong hydrological and trace element imprint [*Hecht*, 1992] that is archived in *G. ruber*. As discussed in more detail in the supporting information, the influence of Ba_{dis} from the coastal area is

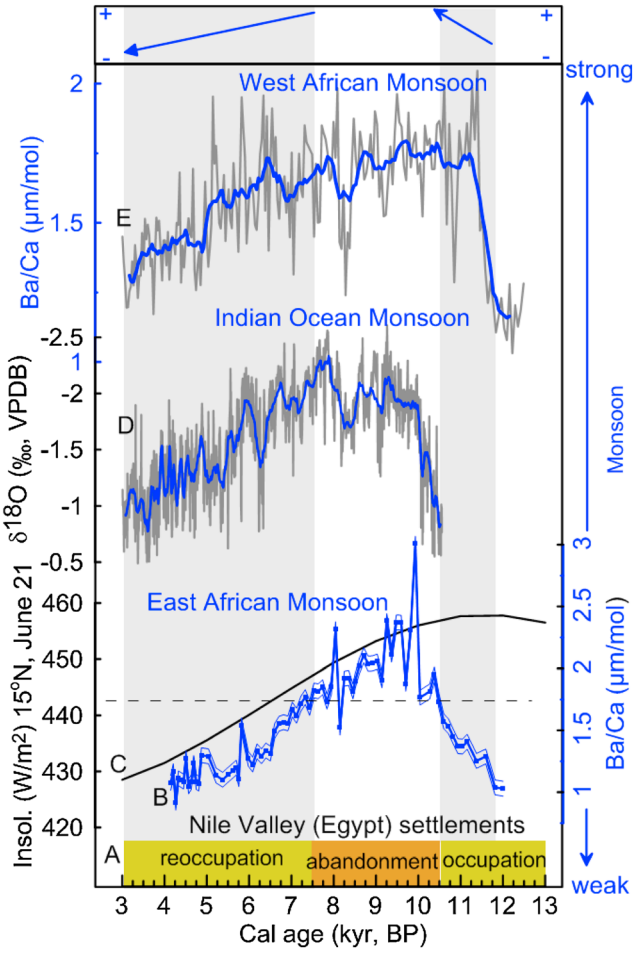

Figure 3. Trend and pace of changes in proxy time series for East African, West African, and Indian Ocean monsoons' hydroclimates. (a) Archeological-based estimate of time windows of prehistoric human occupation and abandonment of river bank settlements in the Nile Valley [*Kuper and Kroepelin*, 2006]. (b) Estimate of Nile runoff based on Ba/Ca analyzed in *G. ruber* pink (this study) considering analytical and time series uncertainties. (c) Orbitally forced changes in insolation [*Berger and Loutre*, 1991]. Dashed line indicates the level of runoff changes that within the age model uncertainty coincide with the timing of abandonment or reoccupation of settlements. (d) $\delta^{18}O$ time series analyzed in stalagmite from Oman indicating changes in Indian Ocean monsoon [*Fleitmann et al.*, 2003]. Bold blue line indicates 11-point running average of highly resolved time series (gray line). (e) Holocene evolution of West African monsoon inferred from Ba/Ca analyzed in *G. ruber* pink from sediment sequence retrieved off large river systems draining the West African monsoon area [*Weldeab et al.*, 2007]. Gray areas and horizontal arrows indicate gradual rise and decline of the Nile River runoff.

negligible due to the absence of local rivers in the vicinity of our core site. Over the last 12 kyr cal B.P., Saharan dust flux over our core site varied between 2 and 6 g/cm^2/kyr with the lowest and highest fluxes occurring during the middle Holocene and pre-Holocene, respectively [*Box et al.*, 2011]. With an average Ba concentration of 400 ppm in Ba-containing phases in Saharan dust [*Moreno et al.*, 2006] and an estimated fractional solubility of 1.5–5% [*Measures et al.*, 2008], the contribution of Saharan dust to Ba_{dis} in the Levantine basin is negligibly low (0.1–0.3 nM). In summary, we cannot exclude minor contribution of Ba_{dis} from the above discussed sources and processes. However, the most dominant factor determining the past variability of Ba/Ca in the Levantine basin is changes in the amount of Nile River discharge. Because of its preference for warm surface water, *G. ruber* in the eastern Levantine basin calcifies primarily during the boreal summer [*Thunell*, 1978]. Therefore, at times of relatively marked seasonal contrast, as is the case today, *G. ruber*'s calcification season would be skewed toward summer and capture surface freshening at the seasonal maximum of Nile River runoff (Figure 1d).

The down-core Ba/Ca record reveals a remarkably gradual transition from a relatively low Nile River runoff and hence weak pre-Holocene EAM to a progressive invigoration of precipitation over the EAM core area (Figure 2). The peak runoff, and by extension the EAM maximum, is centered between 10.1 and 9.1 kyr cal B.P. This observation is consistent with the records of Lake Tana [*Marshall et al.*, 2011] and Lake Victoria [*Berke et al.*, 2012] located in the headwaters of the Blue Nile River and White Nile River, respectively. The abandonment of previously occupied, prehistoric human settlements in the Nile Valley [*Kuper and Kroepelin*, 2006] at the height of Nile runoff (Figure 3) may be not only reflective of climate amelioration in the eastern Sahara [*Kuper and Kroepelin*, 2006] but also likely relates to frequent flooding events of the river banks. While the Nile runoff was still strong, 8.7 kyr cal B.P. marks the onset of a 3500 year period of progressive decline of Nile River runoff, reflecting a markedly gradual weakening EAM precipitation over the Nile basin. Archeological evidence of human reoccupation of settlements in the Nile Valley beginning at 7.5 kyr cal B.P. indicates not only climate deterioration to today's arid northern and central Egypt [*Kuper and Kroepelin*, 2006] but also most likely was facilitated by less hazardous conditions in the Nile Valley due to decline of boreal summer flooding events in response to a EAM weakening.

Starting at 5.3 kyr cal B.P., our record indicates the onset of a low runoff heralding an episode of sustained weak EAM that dominates the late Holocene.

The most salient feature of the Nile River runoff record is the gradual nature of hydroclimate transition between the three markedly different climatic episodes within the Holocene. The transition from dry pre-Holocene to the wet early Holocene occurred in approximately 1800 years. Similarly, the change from wet middle Holocene to relatively dry late Holocene is bridged by a gradual transit that lasted 3500 years. While it is not possible to disentangle the hydrological imprint of the Blue and White Nile Rivers solely on the basis of the Ba/Ca record, hydroclimate reconstructions from Lake Tana [*Marshall et al*., 2011] and Lake Victoria [*Berke et al*., 2012; *Stager et al*., 2003] broadly support the middle to late trend and pace of changes evident in the Ba/Ca record. There is also strong evidence that the middle to late Holocene trend and patterns observed in our spatially integrative runoff record are not limited to the Nile basin. Precipitation over the easternmost part of the Horn of Africa (Somalia and eastern Ethiopia) and the southeastern Arabian Peninsula are fed by western Indian Ocean-sourced moisture that also present a moisture source for precipitation over a significant part of the Nile basin [*Costa et al*., 2014]. Consistent with the pace of the middle to early Holocene transition in our Nile River runoff time series and a model simulation of precipitation over the Horn of Africa [*Renssen et al*., 2006], a hydroclimate record from Lake Chew Bahir in eastern Ethiopia reveals a markedly gradual shift from a wet middle Holocene to a dry Holocene [*Foerster et al*., 2012]. Similarly, the well-dated and highly resolved hydroclimate record from southern Oman [*Fleitmann et al*., 2003] demonstrates that the transition from a humid middle Holocene to the relatively dry late Holocene climate was bridged by a gradual decline of precipitation (Figure 3). Furthermore, reconstruction of dust source and dust flux off Somalia reveals a 2900 year progressive increase of northeast African-sourced dust influx starting at 6.4 kyr cal B.P. that reached its maximum at 3.5 kyr cal B.P. [*Jung et al*., 2004]. Changes in dust mobilization and flux are a response to a complex hydroclimate-vegetation interaction and changes in vegetation pattern [*Claussen et al*., 2013; *Liu et al*., 2007]. Pollen record extracted from a Lake Victoria sediment sequence indicates a gradual decline of trees/shrubs and development of grass vegetation over the last 8000 years [*Kendall*, 1969]. In contrast to the Western Sahara [*Claussen et al*., 2013; *deMenocal et al*., 2000; *Liu et al*., 2007; *Renssen et al*., 2006], the synchronous timing and pacing of changes in precipitation, vegetation, and dust mobilization indicate the absence of nonlinear biogeophysical feedback between changes in precipitation and vegetation in East Africa. A possible explanation for our observation provides the findings of a precipitation and surface albedo model simulation [*Renssen et al*., 2006]. According to the model results [*Renssen et al*., 2006], the late Holocene decline of precipitation in the EAM area did not reach a threshold that would cause large change in vegetation and produce surface albedo strong enough to trigger a nonlinear biogeophysical feedback.

In summary, our spatially integrated hydroclimate record strongly demonstrates that the pace with which the East African climate transitioned from a relatively wet middle Holocene to dry late Holocene was progressive, lasting about 3500 years. The relatively uniform decline of monsoonal precipitation in the northernmost periphery [*Kroepelin et al*., 2008] and Nile basin indicates not only a spatial contraction of precipitation belt but also monsoonal weakening in the EAM core area. A comparison of the middle to late Holocene hydroclimate trend of EAM, as indicated by the Ba/Ca time series, with those of West African [*Weijers et al*., 2007; *Weldeab et al*., 2007] and Indian Ocean monsoons [*Fleitmann et al*., 2003] reveals very similar pacing, indicating that on suborbital timescales all three monsoon systems were sensitive to and driven by a common forcing.

Model simulations indicate that in the absence of meltwater-induced perturbation of the Atlantic meridional overturning circulation (AMOC), the trend and strength of the African monsoon are primarily driven by orbitally forced variation of Northern Hemisphere (NH) summer insolation [*Claussen et al*., 2013; *Kutzbach et al*., 2008; *Liu et al*., 2007; *Marzin et al*., 2013; *Renssen et al*., 2006; *Timm et al*., 2010]. Long EAM proxy-based records overwhelmingly support this hypothesis [*Caley et al*., 2011; *Revel et al*., 2010; *Trauth et al*., 2009; *Ziegler et al*., 2010]. We note that the pace of hydroclimate transition from pre-Holocene to early Holocene is more abrupt in the West African monsoon [*Weldeab et al*., 2007] as compared to that of the EAM (Figure 3). Consistent with the results of model simulation [*Marzin et al*., 2013; *Timm et al*., 2010], we hypothesize that the abruptness of the former is related to a rapid invigoration of the AMOC [*McManus et al*., 2004] and northward expansion of the rain belt following the abrupt termination of the Younger Dryas. In contrast, the gradual strengthening of EAM reflects the influence of moisture advection from the western Indian Ocean that today contributes between 70 and 90% of the moisture advecting into the core area of the Nile basin [*Costa et al*., 2014]. The pace and magnitude of changes in the middle to late Holocene hydroclimatic record of the Nile

basin closely follow the trend of NH summer insolation [*Berger and Loutre*, 1991] and modeled precipitation trend over the Horn of Africa [*Renssen et al*., 2006] (Figure 3). We propose therefore that orbitally forced changes in the NH summer insolation provide the most plausible mechanism in shaping the magnitude and progressive transitions of EAM precipitation during the distinct climatic episodes of the Holocene. Enhanced land-ocean thermal contrast during summer insolation maximum [*Kutzbach et al*., 2008; *Renssen et al*., 2006] is suggested to foster enhanced moisture advection deep into the Nile basin. Strong zonal and interhemispheric moisture advection into the Nile basin due to enhanced moisture recycling over the Congo basin [*Berke et al*., 2012; *Costa et al*., 2014] and strong interhemispheric thermal gradient [*Verschuren et al*., 2009] may have also contributed to the intensification of early to middle Holocene EAM precipitation. As NH summer insolation progressively declined during the middle to late Holocene transition, most likely so did the advection of moisture into the Nile basin. Therefore, we propose that orbitally forced variation of NH summer insolation was the dominant forcing.

The nature of Holocene climate transition in East Africa and the Horn of Africa is controversially debated. The trend of our spatially integrated and hence representative hydroclimate record of East Africa shows no evidence of abrupt early Holocene and middle Holocene climate changes. Consequently, our findings do not support the hypothesis that middle to late Holocene climate transition in East African was abrupt and decoupled from the pace and trend of the West African and Indian Ocean monsoon systems [*Tierney and deMenocal*, 2013]. Instead, the Nile runoff record strongly supports the emerging pattern of Holocene East African middle Holocene climate transition that, consistent with the results of a precipitation-vegetation model simulation [*Renssen et al*., 2006], was marked by gradual hydroclimate and vegetation changes [*Berke et al*., 2012; *Foerster et al*., 2012; *Jung et al*., 2004; *Kendall*, 1969; *Marshall et al*., 2011; *Stager et al*., 2003]. On millennial-to-orbital scale, the synchronous pacing of markedly gradual changes of East African, West African, and Indian Ocean monsoons (Figure 3) indicates that orbitally forced insolation change was the common and dominant forcing.

5. Conclusion

Previous studies are contradictory with regard to the pace of middle to late Holocene East African climate transition. We apply a novel approach and present spatially integrated insights into East African monsoon evolution. The findings of this study demonstrate that the wet to dry Holocene hydroclimate transition in East Africa was markedly progressive and occurred in synchrony with those of the West African and Indian Ocean monsoon climates, pointing to orbitally forced changes in NH summer insolation as the main driver. The pace of hydroclimatic changes in the Nile basin and resulting variation of Nile River level provides an East African climatic context to understand and refine the timing of occupation and abandonment of the settlements in the Nile Valley (Egypt). Furthermore, the synchronous pacing of hydroclimate and vegetation changes as well as dust mobilization in East Africa suggests a linear biogeophysical precipitation-vegetation feedback.

Acknowledgments

S.W. thanks UCSB and the Hellmann Family Foundation for financial supports. V.M. and G.S. acknowledge supports from the Studienstiftung des Deutschen Volkes and the Center of Excellence "Integrated Climate System Analysis and Prediction" (CliSAP) of the Deutsche Forschungsgemeinschaft, respectively. We thank Georges Paradis for ICP-MS operation, James P. Kennett and Dorothy K. Pak for valuable comments on the paper, and Burch Fisher and Deborah Khider for help with map creation and MC simulation, respectively. We also thank the two anonymous reviewers and the handling Editor, Peter Strutton, for their insightful and constructive comments that helped to improved paper.

The Editor thanks two anonymous reviewers for their assistance in evaluating this paper.

References

Almogi-Labin, A., M. Bar-Matthews, D. Shriki, E. Kolosovsky, M. Paterne, B. Schilman, A. Ayalon, Z. Aizenshtat, and A. Matthews (2009), Climatic variability during the last 90 ka of the southern and northern Levantine Basin as evident from marine records and speleothems, *Quat. Sci. Rev.*, *28*(25–26), 2882–2896.

Bahr, A., J. Schönfeld, J. Hoffmann, S. Voigt, R. Aurahs, M. Kucera, S. Flögel, A. Jentzen, and A. Gerdes (2013), Comparison of Ba/Ca and as freshwater proxies: A multi-species core-top study on planktonic foraminifera from the vicinity of the Orinoco River mouth, *Earth Planet. Sci. Lett.*, *383*, 45–57.

Berger, A., and M. F. Loutre (1991), Insolation values for the climate of the last 10 million years, *Quat. Sci. Rev.*, *10*(4), 297–317.

Berke, M. A., T. C. Johnson, J. P. Werne, K. Grice, S. Schouten, and J. S. Sinninghe Damsté (2012), Molecular records of climate variability and vegetation response since the Late Pleistocene in the Lake Victoria basin, East Africa, *Quat. Sci. Rev.*, *55*, 59–74.

Box, M. R., M. D. Krom, R. A. Cliff, M. Bar-Matthews, A. Almogi-Labin, A. Ayalon, and M. Paterne (2011), Response of the Nile and its catchment to millennial-scale climatic change since the LGM from Sr isotopes and major elements of East Mediterranean sediments, *Quat. Sci. Rev.*, *30*, 431–442.

Brovkin, V., and M. Claussen (2008), Comment on climate-driven ecosystem succession in the Sahara: The past 6000 years, *Science*, *322*, 1326.

Caley, T., B. Malaizé, M. Revel, E. Ducassou, K. Wainer, M. Ibrahim, D. Shoeaib, S. Migeon, and V. Marieu (2011), Orbital timing of the Indian, East Asian and African boreal monsoons and the concept of a 'global monsoon', *Quat. Sci. Rev.*, *30*(25–26), 3705–3715.

Claussen, M., and V. Gayler (1997), The greening of the Sahara during the mid-Holocene: Results of an interactive atmosphere-biome model, *Global Ecolo. Biogeogr. Lett.*, *6*, 369–377.

Claussen, M., S. Bathiany, V. Brovkin, and T. Kleinen (2013), Simulated climate–vegetation interaction in semi-arid regions affected by plant diversity, *Nat. Geosci.*, *6*(11), 954–958.

Costa, K., J. Russell, B. Konecky, and H. Lamb (2014), Isotopic reconstruction of the African Humid Period and Congo Air Boundary migration at Lake Tana, Ethiopia, *Quat. Sci. Rev.*, *83*, 58–67.

deMenocal, P., J. Ortiz, T. Guilderson, J. Adkins, M. Sarnthein, L. Baker, and M. Yarusinsky (2000), Abrupt onset and termination of the African Humid Period: Rapid climate responses to gradual insolation forcing, *Quat. Sci. Rev.*, *19*, 347–361.
Edmond, J. M., E. D. Boyle, D. Drummond, B. Grant, and T. Mislick (1978), Desorption of barium in the plume of Zair (Congo) River, *Neth. J. Sea Res.*, *12*, 324–328.
Ehrmann, W., M. Seidel, and G. Schmiedl (2013), Dynamics of Late Quaternary North African humid periods documented in the clay mineral record of central Aegean Sea sediments, *Global Planet. Change*, *107*, 186–195.
Fleitmann, D., S. Burns, M. Mudelsee, U. Neff, J. Kramers, A. Mangini, and A. Matter (2003), Holocene forcing of the Indian Ocean monsoon record in a stalagmite from southern Oman, *Science*, *300*, 1737–1740.
Foerster, V., et al. (2012), Climatic change recorded in the sediments of the Chew Bahir basin, southern Ethiopia, during the last 45,000 years, *Quat. Int.*, *274*, 25–37.
Garcin, Y., A. Junginger, D. Melnick, D. Olago, M. Strecker, and M. H. Trauth (2009), Late Pleistocene-Holocene rise and collapse of the Lake Suguta, northern Kenya Rift, *Quat. Sci. Rev.*, *28*, 911–925.
Gasse, F. (2000), Hydrological changes in the African tropics since the Last Glacial Maximum, *Quat. Sci. Rev.*, *19*, 189–211.
Hamann, Y., W. Ehrmann, G. Schmiedl, and T. Kuhnt (2009), Modern and late Quaternary clay mineral distribution in the area of the SE Mediterranean Sea, *Quat. Res.*, *71*(3), 453–464.
Hamann, Y., S. Wulf, O. Ersoy, W. Ehrmann, E. Aydar, and G. Schmiedl (2010), First evidence of a distal early Holocene ash layer in Eastern Mediterranean deep-sea sediments derived from the Anatolian volcanic province, *Quat. Res.*, *73*(3), 497–506.
Hecht, A. (1992), Abrupt changes in the characteristics of Atlantic and Levantine basin, *Oceanol. Acta*, *15*, 25–42.
Hönisch, B., K. A. Allen, A. D. Russell, S. M. Eggins, J. Bijma, H. J. Spero, D. W. Lea, and J. Yu (2011), Planktic foraminifers as recorders of seawater Ba/Ca, *Mar. Micropaleontol.*, *79*(1–2), 52–57.
Jung, S. J. A., G. R. Davies, G. M. Ganssen, and D. Kroon (2004), Stepwise Holocene aridification in NE Africa deduced from dust-borne radiogenic isotope records, *Earth Planet. Sci. Lett.*, *221*(1–4), 27–37.
Kendall, R. L. (1969), An ecological history of the Lake Victoria basin, *Ecol. Monogr.*, *39*, 121–176.
Kroepelin, S., et al. (2008), Climate-driven ecosystem succession in the Sahara: The past 6000 years, *Science*, *320*(5877), 765–768.
Kuper, R., and S. Kroepelin (2006), Climate-controlled Holocene occupation in the Sahara: Motor of Africa's evolution, *Science*, *313*(5788), 803–807.
Kutzbach, J. E., X. Liu, Z. Liu, and G. Chen (2008), Simulation of the evolutionary response of global summer monsoons to orbital forcing over the past 280,000 years, *Clim. Dyn.*, *30*(6), 567–579.
Lea, D. W. (1990), Foraminiferal and coralline barium as paleoceanographic tracers, PhD thesis, 173 pp., Joint Program in Oceanography, Mass. Inst. of Technol./Woods Hole Oceanogr. Inst., Woods Hole, Mass.
Lea, D. W., and H. J. Spero (1994), Assessing the reliability of paleochemical tracers: Barium uptake in the shells of planktonic foraminifera, *Paleoceanography*, *9*(3), 445–452.
Liu, Z., et al. (2007), Simulating the transient evolution and abrupt change of Northern Africa atmosphere–ocean–terrestrial ecosystem in the Holocene, *Quat. Sci. Rev.*, *26*(13–14), 1818–1837.
Marshall, M. H., H. F. Lamb, D. Huws, S. J. Davies, R. Bates, J. Bloemendal, J. Boyle, M. J. Leng, M. Umer, and C. Bryant (2011), Late Pleistocene and Holocene drought events at Lake Tana, the source of the Blue Nile, *Global Planet. Change*, *78*(3–4), 147–161.
Martin, P. A., and D. W. Lea (2002), A simple evaluation of cleaning procedures on fossil benthic foraminiferal Mg/Ca, *Geochem. Geophys. Geosyst.*, *3*(10), 8401, doi:10.1029/2001GC000280.
Marzin, C., P. Braconnot, and M. Kageyama (2013), Relative impacts of insolation changes, meltwater fluxes and ice sheets on African and Asian monsoons during the Holocene, *Clim. Dyn.*, *41*(9–10), 2267–2286.
McManus, J. F., R. Francois, J.-M. Gherardi, L. D. Keigwin, and S. Brown-Leger (2004), Collapse and rapid resumption of Atlantic meridional circulation linked to deglacial climate changes, *Nature*, *428*, 834–837.
Measures, C. I., W. M. Landing, M. T. Brown, and C. S. Buck (2008), High-resolution Al and Fe data from the Atlantic Ocean CLIVAR-CO2 Repeat Hydrography A16N transect: Extensive linkages between atmospheric dust and upper ocean geochemistry, *Global Biogeochem. Cycles*, *22*, GB1005, doi:10.1029/2007GB003042.
Moreno, T., X. Querol, S. Castillo, A. Alastuey, E. Cuevas, L. Herrmann, M. Mounkaila, J. Elvira, and W. Gibbons (2006), Geochemical variations in aeolian mineral particles from the Sahara-Sahel Dust Corridor, *Chemosphere*, *65*(2), 261–270.
Renssen, H., V. Brovkin, T. Fichefet, and H. Goosse (2006), Simulation of the Holocene climate evolution in Northern Africa: The termination of the African Humid Period, *Quat. Int.*, *150*(1), 95–102.
Revel, M., E. Ducassou, F. E. Grousset, S. M. Bernasconi, S. Migeon, S. Revillon, J. Mascle, A. Murat, S. Zaragosi, and D. Bosch (2010), 100,000 Years of African monsoon variability recorded in sediments of the Nile margin, *Quat. Sci. Rev.*, *29*(11–12), 1342–1362.
Rohling, E. J., P. A. Mayewski, R. H. Abu-Zeid, S. L. Casford, and A. Hayes (2002), Holocene atmosphere-ocean interactions: Records from Greenland and the Aegean Sea, *Clim. Dyn.*, *18*, 587–593.
Saraswat, R., D. W. Lea, R. Nigam, A. Mackensen, and D. K. Naik (2013), Deglaciation in the tropical Indian Ocean driven by interplay between the regional monsoon and global teleconnections, *Earth Planet. Sci. Lett.*, *375*, 166–175.
Schmiedl, G., T. Kuhnt, W. Ehrmann, K.-C. Emeis, Y. Hamann, U. Kotthoff, P. Dulski, and J. Pross (2010), Climatic forcing of eastern Mediterranean deep-water formation and benthic ecosystems during the past 22 000 years, *Quat. Sci. Rev.*, *29*(23–24), 3006–3020.
Sprovieri, M., E. Di Stefano, A. Incarbona, D. Salvagio Manta, N. Pelosi, M. Ribera d'Alcalà, and R. Sprovieri (2012), Centennial- to millennial-scale climate oscillations in the Central-Eastern Mediterranean Sea between 20,000 and 70,000 years ago: Evidence from a high-resolution geochemical and micropaleontological record, *Quat. Sci. Rev.*, *46*, 126–135.
Stager, J. C., B. F. Cumming, and L. D. Meeker (2003), A 10,000-year high-resolution diatom record from Pilkington Bay, Lake Victoria, East Africa, *Quat. Res.*, *59*(2), 172–181.
Thunell, R. (1978), Distribution of recent planktonic foraminifera in surface sediments of the Mediterranean Sea, *Mar. Micropaleontol.*, *3*, 147–173.
Tierney, E. J., and B. P. DeMenocal (2013), Abrupt shift in Horn of Africa hydroclimate since the last glacial, *Science*, *342*, 842–846.
Timm, O., P. Köhler, A. Timmermann, and L. Menviel (2010), Mechanisms for the Onset of the African Humid Period and Sahara Greening 14.5–11 ka BP*, *J. Clim.*, *23*(10), 2612–2633.
Trauth, M. H., J. C. Larrasoaña, and M. Mudelsee (2009), Trends, rhythms and events in Plio-Pleistocene African climate, *Quat. Sci. Rev.*, *28*(5–6), 399–411.
Ufkes, E., J. H. Fred Jansen, and G.-J. A. Brummer (1998), Living planktonic foraminifera in the eastern South Atlantic during spring: Indicators of water masses, upwelling and the Congo (Zaire) River plume, *Mar. Micropaleontol.*, *33*(1–2), 27–53.
Verschuren, D., J. S. Sinninghe Damste, J. Moernaut, I. Kristen, M. Blaauw, M. Fagot, G. H. Haug, and C. p. members (2009), Half-precessional dynamics of monsoon rainfall near the East African Equator, *Nature*, *462*(7273), 637–641.

Webster, P. J., A. M. Moore, J. P. Loschnigg, and R. R. Leben (1999), Coupled ocean-atmosphere dynamics in the Indian Ocean 1997-98, *Nature*, *401*, 356–360.

Weijers, J. W., E. Schefuss, S. Schouten, and J. S. Sinninghe Damste (2007), Coupled thermal and hydrological evolution of tropical Africa over the last deglaciation, *Science*, *315*(5819), 1701–1704.

Weldeab, S. (2012), Bipolar modulation of millennial-scale West African monsoon variability during the last glacial (75,000–25,000 years ago), *Quat. Sci. Rev.*, *40*, 21–29.

Weldeab, S., D. W. Lea, R. R. Schneider, and N. Andersen (2007), 155,000 years of West African monsoon and ocean thermal evolution, *Science*, *316*(5829), 1303–1307.

Weldeab, S., M. Frank, T. Stichel, B. Haley, and M. Sangen (2011), Spatio-temporal evolution of the West African monsoon during the last deglaciation, *Geophys. Res. Lett.*, *38*, L13703, doi:10.1029/2011GL047805.

Ziegler, M., E. Tuenter, and L. J. Lourens (2010), The precession phase of the boreal summer monsoon as viewed from the eastern Mediterranean (ODP Site 968), *Quat. Sci. Rev.*, *29*(11–12), 1481–1490.